Journal of Chromatography, 325 (1985) 137–149
Elsevier Science Publishers B.V., Amsterdam — Printed in The Netherlands

CHROM. 17 620

SIMPLE UV ABSORPTION DETECTOR FOR CAPILLARY ISOTACHOPHORESIS*

P. HAVAŠI* and D. KANIANSKY
Institute of Chemistry, Komenský University, Mlynská dolina CH-2, CS 842 15 Bratislava (Czechoslovakia)
(First received October 18th, 1984; revised manuscript received January 8th, 1985)

SUMMARY

A fixed-wavelength UV absorption on-column detector suitable for capillary isotachophoresis was developed. Its simple construction, small dimensions and cheapness were achieved without sacrificing the analytical performance. The detector was designed as a single-beam modular unit consisting of a contactless gas discharge lamp, interference filter, rectangular slit system and a semiconductor photosensor with enhanced UV sensitivity through the use of a luminescence wavelength shifter. The lamp is powered by a high-frequency oscillator of reliable performance with small dimensions for its use in the on-column configuration of the detector. A detailed description of the mechanical arrangement of the detector and its electronic circuitry is given. The results of performance tests, which are of interest from the point of view of analytical isotachophoresis, are also given.

INTRODUCTION

UV absorption detectors operating at a fixed wavelength are currently used as selective detectors in capillary isotachophoresis (ITP). Their analytical advantages, especially in conjunction with high-resolution conductivity or potential gradient detectors, are well recognized[1,2].

The design of these detectors differs in several important respects from that of photometric flow-through detectors as used, *e.g.*, in liquid chromatography (LC). In particular, the cell volumes of the detectors employed for ITP must be considerable smaller, even in comparison with those currently used in micro high-performance LC (*e.g.*, refs. 3–6) or in open-tubular LC[7–10]. For example, 2–6 nl cell volumes are required for 0.2 mm I.D. tubes to exploit the analytical capabilities of ITP[11–13].

On-column absorption detectors are essential in ITP[1,11–13], and their use also seems advantageous for LC in open-tubular columns, as recently shown by Guthrie and Jorgenson[14]. However, the use of focusing optics designed for large-volume

* Presented at the *4th International Symposium on Isotachophoresis, Hradec Králové, September 2–6, 1984*. The majority of the papers presented at this symposium have been published in *J. Chromatogr.*, Vol. 320, No. 1 (1985).

0021-9673/85/$03.30

detection cells causes some problems in on-column LC absorption detectors having cell volumes of 20 nl or less[15]. With respect to higher concentrations of the constituents present in isotachophoretically migrating zones, the design of the absorption detectors for ITP may not solve these problems, even for smaller cell volumes.

A detailed description of a fixed-wavelength detector suitable for ITP was given by Everaerts *et al.*[1]. In spite of the fact that information concerning the construction of other UV detectors developed for ITP is scarce or available only from the manufacturers' service manuals, their design seems to follow an arrangement similar to that proposed by Everaerts *et al.*

The aim of this work was to develop a simple, cheap, on-column UV absorption detector suitable for ITP and having performance characteristics that meet the current analytical requirements of the technique. For these reasons we had to follow the requirements of ITP rather than to design a universally applicable UV absorption detector. However, its potential in other fields, *e.g.*, capillary zone electrophoresis, LC and flow injection analysis, can be estimated from the performance characteristics presented here.

RESULTS AND DISCUSSION

Detector design principles

To follow our main design aims, the use of optical components such as lenses, mirrors and optical fibres was excluded. Instead, we preferred to use a tight "sandwich" arrangement of the detector system consisting of a contactless low-pressure discharge lamp – interference filter – capillary tube system with slits – detection sensor. Also, a single beam configuration was preferred for the same reasons. We found that such an arrangement of the detector provides sufficient light intensity for reliable detection during ITP analysis.

It is known that the gas discharge lamp of the detector can be powered continuously or in a chopper mode. The use of a chopper mode with synchronous detection of the signal from the sensor can be advantageous as both the drift of the detection system and stray light effects are reduced. On the other hand, a decrease in the signal-to-noise ratio can obviate these advantages of the chopper mode (ref. 1, p. 159). Therefore, we decided to use a simpler continuous mode with non-modulated detection.

Light source

A contactless, low-pressure mercury (Hg–Ar) discharge lamp was chosen as the light source at 254 nm. For detection at 206, 280 or 340 nm an iodine lamp of the same type can be used[11,16]. We preferred this type of lamp as it is simple to manufacture (ref. 1, p. 155) and the lifetime of, *e.g.*, an Hg–Ar lamp is claimed to be 6000 working hours[17]. We found experimentally that the intensity of the 253.7 nm spectral line of the Hg–Ar lamp (constructed using the procedure described in ref. 1 or obtained commercially as an LKB UV lamp Type 2) is considerably higher in the direction perpendicular to the axis of the lamp. However, to our knowledge, discharge lamps of this construction are placed in detectors for ITP in such a way that the axis of the lamp is identical with the optical axis of the detection system (*i.e.*, in the direction providing less UV light). For obvious reasons, in our design we used the position of the lamp giving higher light intensities (see below).

A basic requirement for reliable excitation of a contactless discharge lamp is to keep a high field strength of a high frequency (H.F.) electric field between the plates of the excitation capacitor. By far the best results were achieved with an H.F. power oscillator developed for this purpose in our laboratory (Fig. 5). The light intensity of the Hg–Ar lamp increased when it was kept at an optimal temperature (40°C in this work). This could be expected in view of the strong dependence of the light intensity of low-pressure Hg lamps on temperature[18].

Detection cell with filter system

In practice, the photometric detection cell in ITP is formed by a slit system mounted directly on the capillary tube used for the separation (*e.g.*, refs. 1 and 13) or by fibre optics[13,19]. Slits of circular cross-section (0.1–0.3 mm diameter) seem to be used exclusively in detectors for ITP. The cell volumes vary in the range 1–20 nl depending on the dimensions of the slit and the inner diameter of the capillary tube. For obvious reasons the slit width in the direction along the capillary axis should be as small as possible in order to detect very short UV light-absorbing zones. On the other hand, a signal of good quality provided by the detection element is desirable. These opposing requirements determine the geometrical dimensions of the slit. In practice, however, circular slits with a diameter as small as 0.1 mm provide very satisfactory results[11–13]. Only circular slits would appear to be used in the detectors for ITP. As the technology needed to manufacture rectangular slits is simpler than that used for circular slits of very small diameter, we calculated the responses of the detector for slits of these cross-sections (for an ideal zone boundary moving in both instances at the same velocity) in order to compare their distinctions in this respect. Both the zone boundary profiles and the varying thickness of the solution layer within the slit were neglected in these calculations. In spite of the fact that these effects must be taken into account when precise calculations are required, their neglect for our purposes was reasonable.

For the calculations of the response of the detector for a circular slit the following equation was used:

$$S_C(T) = KT\sqrt{\frac{D^2}{4} - K^2T^2} + \frac{D^2}{4}\arcsin\left(2\frac{KT}{D}\right) + \frac{\pi D^2}{8}$$

$$T \in \left[-\frac{D}{2K}; \frac{D}{2K}\right]$$

where S_C is the area of the circular slit, D is its diameter, K is the constant migration velocity and T is time. For a rectangular slit the following equation applies:

$$S_R(T) = K\,D\,T$$

$$T \in \left[0; \frac{d}{K}\right]$$

where S_R is the area of the rectangular slit and D and d are its width and height, respectively.

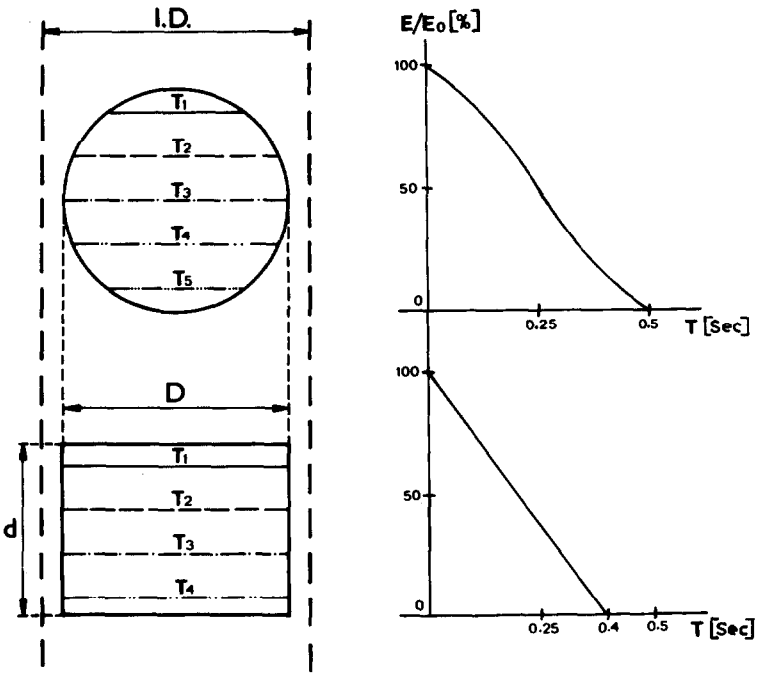

Fig. 1. Comparison of the responses of a photometric detector with circular and rectangular slits for an ideal zone boundary migrating isotachophoretically. Slits of the same area are compared. The response curves were calculated for $D = 0.25$ mm and $v_{iso} = 0.5$ mm/sec. T_1–T_5 = positions of the zone boundary in the slits for different times. For further details, see the text.

When slits of both cross-sections having the same area are compared (see Fig. 1), we obtain the following equation:

$$d = \frac{\pi D}{4}$$

This means that for a given diameter (D) of the circular slit the height of the equivalent rectangular slit (d) is *ca.* 78% of D. In other words, a rectangular slit provides better detection possibilities (when the above assumptions hold). These facts are illustrated in Fig. 1. Although the calculations were not examined by precise measurements, they at least justify the use of a rectangular slit in our design. The final solution for the slit system is shown below.

The desired wavelength of the incident light in absorption detectors for ITP is selected by an interference filter combined with an end filter[1,20]. This filter system is placed between the exit slit and a photosensing element. The light spectrum of a low-pressure Hg–Ar discharge lamp is poor and the 253.7 nm line provides *ca.* 90% of the total energy irradiated in the 200–700 nm region. For this reason, the use of a cheap end filter to "monochromate" the light beam was tested in our laboratory. This solution was omitted in the final detector design as stray light effects due to weak spectral lines of the lamp in the UV region would be unavoidable[21]. Instead,

a small-diameter 254 nm interference filter having a 25 nm bandwidth was used. To decrease the energy with which the capillary tube is irradiated [in our work a 0.30 mm I.D. tube made of fluorinated ethylene–propylene copolymer (FEP)], we placed the filter between the light source and the inlet slit. As the total energy output of the lamp used is relatively small, no heat protection of the filter was necessary[14].

Detection sensor

Vacuum phototubes[1,11–13], photomultipliers[22] or a UV-sensitive silicon photocell[23] are the photosensing elements used in UV detectors for ITP.

To achieve a cheap solution for the detection part, we used a current phototransistor and its enhanced UV sensitivity was achieved through luminescent conversion of the incident light. An analogous idea is employed in quantum counters (*e.g.*, refs. 24 and 25). In our design a highly efficient luminophore (283 De Luxe; Sylvania, U.S.A.) having the emission maximum at 640 nm served for the light conversion. Maximum collection efficiency of the emitted light[26] by the phototransistor was achieved by applying a thin layer of the luminescent material on its window (see Fig. 2).

If a *ca.* 50% collection efficiency (a reasonable estimate from the geometrical arrangement) and a 80–90% conversion rate[27] are assumed, then 40–45% of the UV light passing through the detection cell enters the photosensitive element converted to light of wavelengths that coincide well with its radiant sensitivity.

We believe that such a solution for the detection sensor could be also useful,

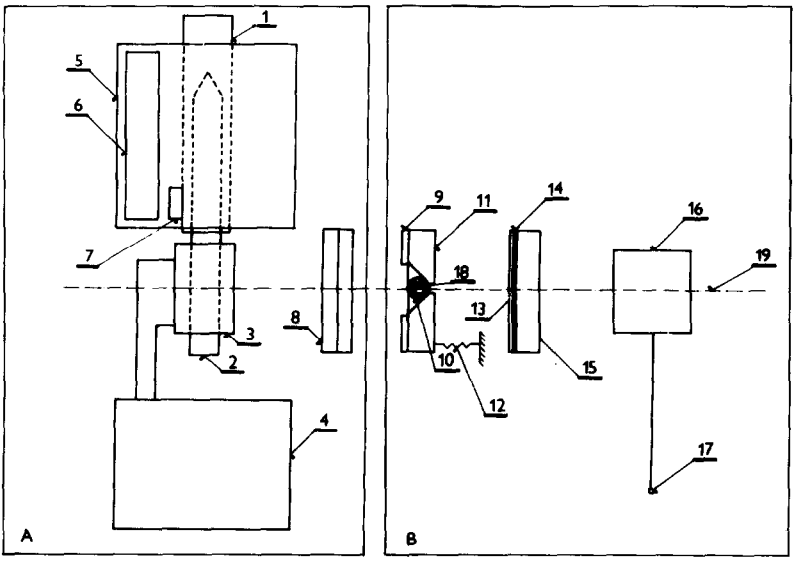

Fig. 2. Mechanical arrangement of the on-column part of the detector. A = Exchangeable module; B = module permanently mounted on the column. 1 = Lamp holder; 2 = contactless low-pressure Hg–Ar lamp; 3 = excitation electrodes; 4 = high-frequency power oscillator; 5 = thermostated block; 6 = heating element; 7 = thermistor; 8 = 254 nm interference filter; 9 = input slit; 10 = FEP capillary tube; 11 = capillary bed with the output slit; 12 = spring fixing the capillary tube in the bed (11); 13, 15 = PTFE foils; 14 = wavelength shifter; 16 = Si phototransistor; 17 = output from the detector; 18 = detection cell; 19 = optical path. For a detailed description, see the text.

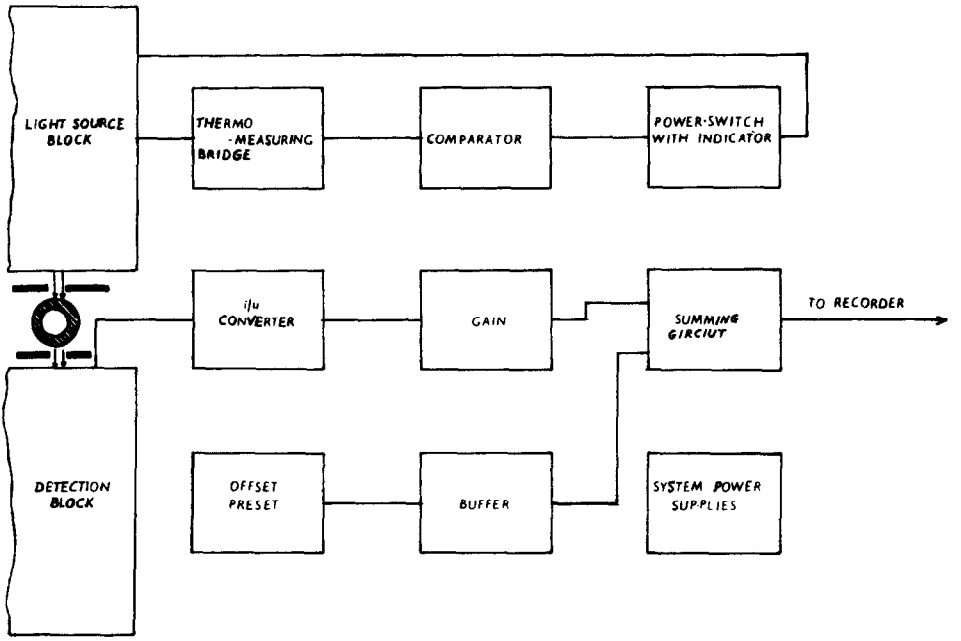

Fig. 3. Schematic diagram of the electronics of the detector.

e.g., for detection at 206 nm[11,16], where the responses of current UV detector elements are low.

This design of the detection element also simplifies the electronics employed for the signal processing and the detection part can be of small dimensions for on-column mounting.

Mechanical construction

The detector was constructed as a unit consisting of two subunits (Figs. 2 and 3). The first subunit includes a thermostated Hg–Ar discharge lamp, an interference filter with its holder, slit system, sensor, H.F. power oscillator and a current–voltage converter. This part is placed in a housing that is mounted on the column. The second subunit of the detector, which includes the remainder of the electronic circuits, is placed in a separate case.

The on-column subunit consist of two modules (A and B in Fig. 2). Module B is permanently mounted on the column whereas module A is exchangeable. Both modules are clamped tightly by screws and a miniature connector serves as an electric connection. The lamp 2 in Fig. 2 is removable from its working position by axial pulling and its mechanical stability during the measurement is achieved by a simple ball-lock (not shown in Fig. 2). For the reason mentioned above the axis of the lamp, when placed between two excitation electrodes, is perpendicular to the optical axis of the detector (dash and dot line in Fig. 2). An exchangeable interference filter (8) and the lamp are placed tightly against the input slit (9) to maximize the intensity of the light passing through the detection cell.

The capillary tube (10) is fixed in a groove made of duralumin (11) by two 0.1

mm thick stainless-steel foils. A spring (12) provides tight and gentle fixing of the tube in the groove. The output slit is also made from two stainless-steel foils of 0.1 mm thickness. These foils are placed on the rear side of the groove (11) in such a way that the distance (in the direction of the capillary axis) between their neighbouring margins determines the height of the slit. The width of the slit is determined by the groove alone (see Fig. 2). In this work we used an output slit of height 0.2 mm and width 0.3 mm. An input slit of larger dimensions was made in the same way. Using this type of capillary holder, we could insert the tube in the groove in the desired manner and very reproducibly. Also, cleaning of the outer wall of the tube in the detection position (*e.g.*, to remove dust particles) can be carried out very easily.

A KPX 81 phototransistor (Tesla, Piešťany, Czechoslovakia) was used as a sensor (16 in Fig. 2). However, any other equivalent of this element, *e.g.*, BPX 81 (Siemens, Munich, F.R.G.) can be used for this purpose. The KPX 81 has a square radiation-sensitive area (0.4 × 0.4 mm) at the base–emitter junction and it has similar dimensions to the outlet slit. The luminophore was used as a very thin layer (14) fixed from both sides by polytetrafluorethylene foils of 0.01 mm thickness and tightly clamped on to the input window of the phototransistor by a pair of thin-walled metallic tubes.

Detector electronics

A schematic diagram of the electronics of the developed detector is given in

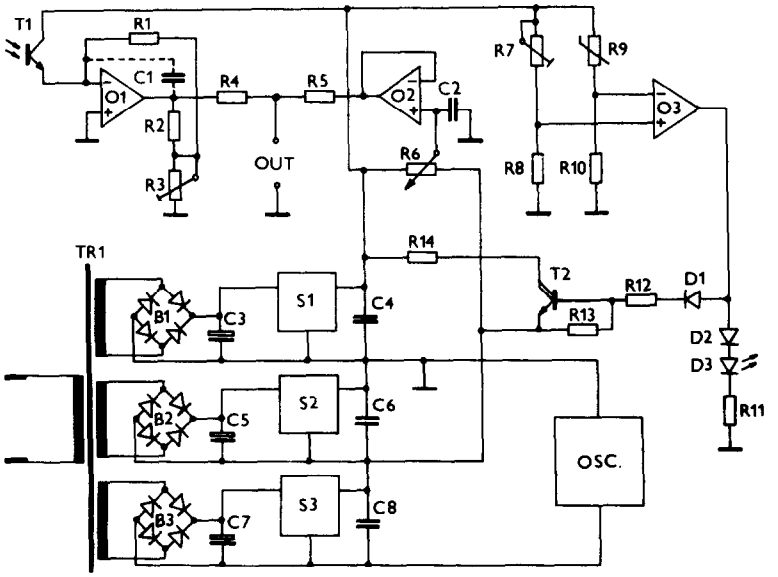

Fig. 4. Electronic circuit of the UV absorption detector. Semiconductor components: 01 = MAC 156, 02–03 = MAA 741C; T1 = KPX 81; T2 = KD 367; B1–B3 = KY 130/150; S1–S2 = MA 7815; S3 = MA 7824; D1–D2 = KY 130/180; D3 = LQ 100 LED (all components were obtained from TESLA, Rožnov, Czechoslovakia). Metal film resistors (1/4 W, 5%): R1 = 10 MΩ; R2–R5 = 10 kΩ; R8 = 1 kΩ; R10–R12 = 1 kΩ; R13 = 470 Ω. Potentiometers: R3 = 220 Ω; R6 = 10 kΩ; R7 = 10 kΩ; R9 = 4.7 kΩ; negative temperature coefficient thermistor. Capacitors: C1 = 100 pF (ceramic); C2 = 1 μF (polyester); C3, C5, C7 = 500 μF (electrolyte); C4, C6, C8 = 0.1 μF (ceramic). TR1 = 40 W power transformer (core size 25 × 25 mm). For further details, see the text.

Fig. 3 and the complete electronics of the detection part are shown in Fig. 4. The detection phototransistor (T1 in fig. 4), which provides currents in the range 10^{-10}–10^{-7} A, is connected to the input of the operational amplifier (01) which serves as a current–voltage converter. Any operational amplifiers provided with J-FET input buffers can be used for this purpose. The gain of this converter is adjustable by the potentiometer R3. A feedback capacitor (C1) serves for noise filtration. It was omitted from our instrument, however, as the filtration ability of the recorder used (TZ 4200; Laboratorní Přístroje, Prague, Czechoslovakia) was sufficient. The operational amplifier (02) serves as a source follower and buffers the offset potentiometer R6. The voltages on the outputs of 01 and 02 are summed by the summing resistors R4 and R5. The resulting voltage is led to an output connector (OUT).

Resistors R7, R8 and R10 and a thermistor with a negative temperature coefficient of resistance R9 form a thermometric bridge. The balance of this bridge is evaluated by a comparator (03) which controls a heat resistor (R14). The status of the thermostat is indicated by an LED diode (D3). The electronics are powered by standard power supplies provided with integrated monolithic voltage stabilizers (S1–S3). For further details, see the legend to Fig. 4.

An H.F. power oscillator operating at approximately 50 MHz was developed for the present UV detector. It has several advantages in comparison with other arrangements. Its circuit is shown in Fig. 5.

An H.F. power transistor is coupled to a common collector. This permits perfect cooling of the transistor because most of the H.F. transistors have the collector coupled to their metal caps. The resonant frequency of the oscillator is determined by an inductance (2, Fig. 5) and a capacitor (3), which form a series resonant circuit

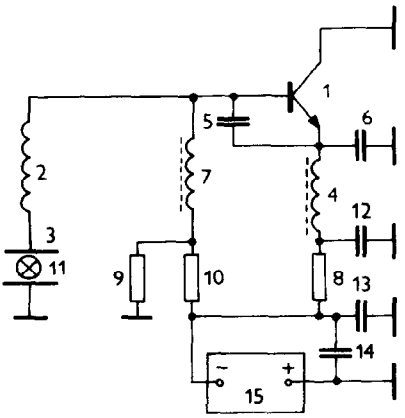

Fig. 5. High-frequency power oscillator. 1 = High-frequency power transistor (KF 508); 2 = resonant inductance (air type, 13-turn coil of 25 mm diameter wound from a 0.8 mm diameter silver-coated copper wire covered with an FEP insulation tube); 3 = resonant capacitor (two 10 × 25 mm Ni-plated copper foils of 0.5 mm thickness fixed by PTFE holders; the distance between the electrodes is 10 mm); 4, 7 = ferrite choke (15-turn coil wound of a 0.3 mm diameter insulated copper wire; cylindrical ferrite core of 4 mm diameter); 5 = ceramic capacitor (120 pF); 6 = ceramic capacitor (27 pF); 8 = metal film resistor (39 Ω, 0.25 W, 5%); 9 = metal film resistor (470 Ω, 0.25 W, 5%); 10 = metal film resistor (0.25 W, 5%, the proper value must be chosen in accordance with the transistor used); 11 = gas discharge lamp; 12 = ceramic capacitor (10 nF); 13 = feed-through capacitor (3.3 nF); 14 = ceramic capacitor (10 nF); 15 = 40 V/150 mA d.c. power supply.

in this instance. If a high quality factor of the inductance is attained (by suitable construction) and if the series resonant circuit is in resonance with a frequency from an ideal voltage generator supplying the series resonant circuit, the amplitudes of the H.F. voltages present on the inductance and capacitance of this circuit are the quality factor times higher than the amplitude of the generator voltage (for the best quality of the capacitance). For example, for an inductance having a quality factor of 150 and for a frequency of $5 \cdot 10^7$ Hz, we can expect an approximately 6000 V amplitude on both the inductance and capacitance of the series resonant circuit for a 40 V amplitude of the voltage generator. When a gas discharge lamp is placed between the plates of such a capacitance, we can expect its immediate and reliable excitation. The oscillator shown in Fig. 5 is of the Gouriet–Clapp type. Its proper function is achieved through the selection of the capacitance divider (5 and 6 in Fig. 5). The voltage generator consists of a KF 508 H.F. power transistor (Tesla, Piešťany, Czechoslovakia) and of an emitter choke (4) and capacitance divider (5 and 6). The proper working position of the transistor (1) is pre-set by a resistor divider (9 and 10) and it is separated from its base by a choke (7).

In our detector, the oscillator is placed in a metallic housing (iron with a tin-coated surface). Small geometrical dimensions of this housing (50 × 35 × 15 mm, which is comparable, *e.g.*, to a box of matches) enabled us to reduce the dimensions of the on-column part of the detector substantially. The excitation capacitor placed in module A (Fig. 2) is coupled to the oscillator (placed in module B, Fig. 2) through a miniature high-voltage connector. The negative pole of a d.c. power supply is coupled to the oscillator box by a feed-through capacitor (13, Fig. 5), while the positive pole is identical with the electrical earth of the electronic circuitry.

Excellent reliability of the oscillator was confirmed by long-term testing (*ca.* 2500 h) without observable darkening of the lamps.

Performance evaluation

For the performance evaluation of the detector, ASTM (American Society for Testing and Materials) standard practice for testing fixed-wavelength photometric detectors used in LC[28,29] served as a guide. With respect to the methodological differences between LC and ITP, some of the proposed performance parameters (*e.g.*, flow sensitivity, time interval used for the short-term and long-term noise measurements) were omitted or modified according to the requirements of ITP.

The response characteristics of the detector at 254 nm were measured for aqueous solutions of sodium benzoate within the concentration range $0–10^{-1}$ *M*. As the detector was not provided with a logarithmic converter, the values measured on the transmittance scale were converted into absorbance values. The solution in the capillary did not move during the measurements as is common in ITP. Three series of measurements were carried out within 3 days with the same solutions. For each series of measurements the warm-up time for the detector was *ca.* 3 h. The response curve for the detector at 254 nm (Beer–Lambert plot) is given in Fig. 6.

The short-term noise in LC[28,29] is defined as random variations (in absorbance units, A.U.) with a frequency higher than 1 cycle/min and its measurement should be carried out over a 15 min time interval. The short-term noise in LC determines the smallest signal detectable by a photometric detector, limits the precision attainable in the quantitation of trace samples and sets the lower limit of linearity. In ITP

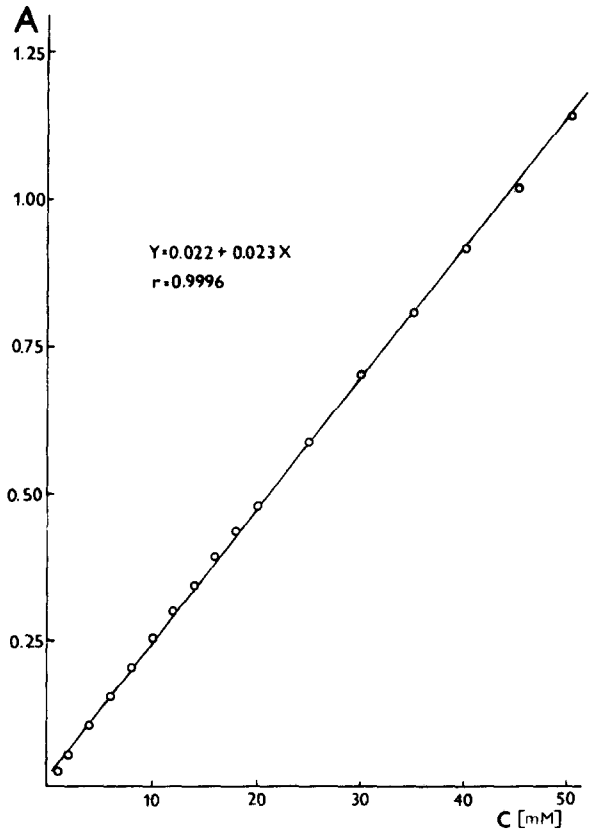

Fig. 6. Response characteristics of the detector at 254 nm. The procedure for the measurements is described in the text. A linear relationship describing the response characteristics was evaluated from 51 calibration points.

this performance parameter should mainly determine the limit of detection of constituents present as spikes[1,2,30,31] and provide information concerning the precision attainable in quantitative analysis either from spike peak-height or peak-area measurements. For these reasons our short-term noise measurements were carried out over 2 min time intervals for a capillary tube filled with water. Each pair of parallel lines defining the envelope of all recorded variations corresponded to 20–30 sec (for details see refs. 28 and 29). The mean value of the short-term noise evaluated in this manner was 0.0007 A.U. (0.0001 A.U. standard deviation) for a 0.30 mm I.D. capillary tube (0.17 mm wall thickness) made of FEP. This value is in good agreement with that reported by Reijenga *et al.*[13].

The long-term noise in LC represents the noise that can be mistaken for a late-eluting peak[28,29]. Such an interpretation is meaningless in ITP. Instead, it can define the limits with which the purity of the zone can be detected at a given wavelength and it can also determine the precision of quantitative analysis obtained from the steady-state mixed zones[32,33]. In ITP the residence time of a migrating zone in the detector is only very seldom longer than 2–3 min. Therefore, we evaluated the

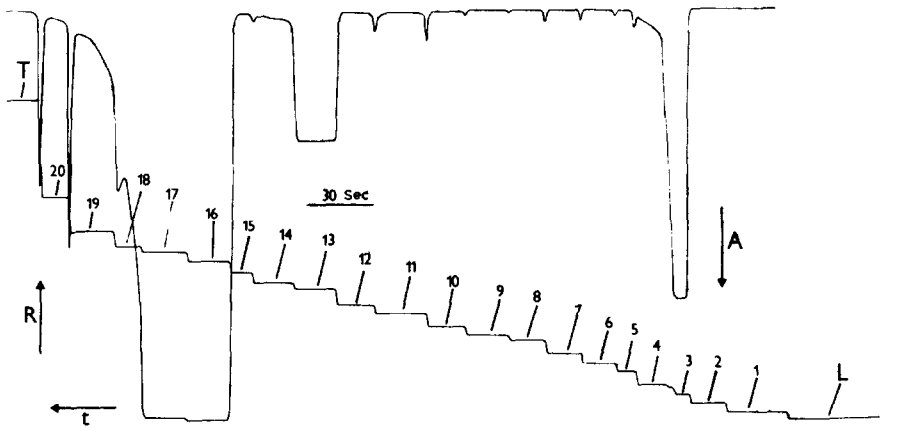

Fig. 7. Isotachopherogram for the analysis of an anionic test mixture at pH 6.0. The separation was performed in a home-made column-coupling instrument[35]. The responses of both conductivity and UV (254 nm) detectors from the analytical column only are given. 1 = Sulphuric; 2 = chloric; 3 = chromic; 4 = malonic; 5 = succinic; 6 = glutaric; 7 = adipic; 8 = glycolic; 9 = acetic; 10 = dichloroacetic; 11 = lactic; 12 = β-bromopropionic; 13 = benzoic; 14 = butyric; 15 = aspartic; 16 = sorbic; 17 = cinnamic; 18 = glutamic; 19 = enantic; 20 = α-aminoadipic acid. L = Chloride (used at a 10 m*M* concentration in the leading electrolyte); T = morpholinoethanesulphonic acid; histidine was used as a counter ion and 0.1% hydroxyethylcellulose was added to the leading electrolyte. The driving current during the run in the analytical column was 45 μA.

long-term noise of the detector for 10 min time intervals. Using the procedure described for LC, we obtained a value of 0.001 A.U. for the long-term noise (the mean of five measurements carried out within 3 days) when the measuring conditions were the same as in the short-term noise measurements.

Analysis of a model mixture of ionic constituents using the developed detector is shown in Fig. 7. The photometric detector was mounted *ca.* 20 mm up-stream of the conductivity detector[34].

Some of the zones as registered by the UV detector show tailing (chromate, cinnamate). The causes of this phenomenon in ITP (see, *e.g.*, the analyses of some model mixtures in ref. 1) are not yet clear. However, it cannot be ascribed to a high time constant of the detector–recorder system (ca. 0.1 sec in this instance). The presence of impurities in the electrolyte solutions, the existence of mixed zones of some microconstituents with separands present at higher concentrations, reactions of UV light-absorbing constituents or slow desorption of the separands from the capillary wall could be responsible for the tailing. It is obvious that a detailed investigation is necessary in order to obtain an explanation, which is probably different for different separands.

CONCLUSIONS

This thorough examination of the factors important for the design of a fixed-wavelength UV absorption detector for ITP enabled us to develop a single and cheap modular detection device that meets the current analytical requirements of the technique.

A contactless low-pressure mercury lamp powered by a substantially simplified H.F. power oscillator provides a reliable light source at 254 nm. Undoubtedly, other lamps of this type suitable for other wavelengths can be employed for the detection of separands in conjunction with proper interference filters. Experiments performed recently in our laboratory with a mercury discharge lamp employed in sun-lamps showed the suitability of this cheap and reliable UV light source for our UV absorption detector.

The simple holder of the capillary tube enables one to choose an output rectangular slit of the desired dimensions while the tube can be fixed very reproducibly. A detection sensor employing a current phototransitor with a solid luminescent wavelength shifter provides sufficient detection sensitivity, minimizes the geometrical dimensions and simplifies the design of the whole detector.

The noise parameters of the detector (0.0007 and 0.001 A.U. for the short- and long-term noise, respectively) enable one to calculate the detection limits and the reproducibilities attainable for separands under the conditions of ITP separations in a 0.3 mm I.D. FEP capillary tube.

ACKNOWLEDGEMENT

The authors thank Dipl. Ing. Stanislav Alakša of Tesla, Piešťany, Czechoslovakia, for valuable advice and suggestions.

REFERENCES

1 F. M. Everaerts, J. L. Beckers and Th. P. E. M. Verheggen, *Isotachophoresis: Theory, Instrumentation and Applications*, Elsevier, Amsterdam, Oxford, New York, 1976.
2 S. G. Hjalmarsson and A. Baldesten, *CRC Crit. Rev. Anal. Chem.*, 11 (1981) 261.
3 D. Ishii, K. Asai, K. Hibi, T. Jonokuchi and M. Nagaya, *J. Chromatogr.*, 144 (1977) 157.
4 R. P. W. Scott, *J. Chromatogr. Sci.*, 18 (1980) 49.
5 T. Takeuchi and D. Ishii, *J. Chromatogr.*, 239 (1982) 633.
6 V. L. McGuffin and M. Novotný, *J. Chromatogr.*, 255 (1983) 381.
7 D. Ishii and T. Takeuchi, *J. Chromatogr. Sci.*, 18 (1980) 462.
8 M. Novotný, *J. Chromatogr. Sci.*, 18 (1980) 473.
9 M. P. Maskarinec, J. D. Vargo and M. J. Sepaniak, *J. Chromatogr.*, 261 (1983) 245.
10 P. Kucera and G. Guiochon, *J. Chromatogr.*, 283 (1984) 1.
11 J. C. Reijenga, *Thesis*, University of Technology, Eindhoven, 1984.
12 J. C. Reijenga, G. V. A. Aben, Th. P. E. M. Verheggen and F. M. Everaerts, *J. Chromatogr.*, 260 (1983) 241.
13 J. C. Reijenga, Th. P. E. M. Verheggen and F. M. Everaerts, *J. Chromatogr.*, 267 (1983) 75.
14 E. J. Guthrie and J. Jorgenson, *Anal. Chem.*, 56 (1984) 483.
15 S. R. Abbott and J. Tusa, *J. Liq. Chromatogr.*, 6 (1983) 77.
16 Th. P. E. M. Verheggen, F. M. Everaerts and J. C. Reijenga, *J. Chromatogr.*, 320 (1985) 99.
17 *LKB 2138 Uvicord S*, Publication No. 2138-E02, LKB, Bromma, 1979.
18 Š. Kubín, *Zdroje Fotosynteticky Účinného Záření a Metody jeho Měření*, Academia, Prague, 1973, p. 97.
19 *Improved Conductivity Detector 2127-140*, LKB, Bromma, 1977.
20 *LKB 2127 Tachophor*, Instrument Manual, LKB, Bromma, 1977.
21 A. Wiese, B. Dehmer, T. Dörr and G. Hörschele, *Hewlett-Packard J.*, 35 (1984) 27.
22 Z. Prusík, Institute of Organic Chemistry and Biochemistry, ČSAV, Prague, personal communication.
23 *Basic Isotachophoresis*, CA 198-905 B, Shimadzu, Tokyo, 1981.
24 J. Yguerabide, *Rev. Sci. Instrum.*, 39 (1968) 1048.
25 J. N. Demas and G. A. Crosby, *J. Phys. Chem.*, 75 (1971) 991.

26 H. A. Strobel, *Chemical Instrumentation*, Addison-Wesley, Reading, Menlo Park, London, 2nd ed., 1973, p. 423.
27 K. Pátek, *Luminescence*, SNTL, Prague, 1962.
28 T. Wolf, G. Fritz and L. R. Palmer, *J. Chromatogr. Sci.*, 19 (1981) 387.
29 *Standard Practice for Testing Fixed-Wavelength Photometric Detector Used in Liquid Chromatography*, ANSI/ASTM E 685-79, American Society for Testing and Materials, Philadelphia, 1979.
30 L. Arlinger, *J. Chromatogr.*, 91 (1974) 785.
31 M. Svoboda and J. Vacík, *J. Chromatogr.*, 119 (1976) 539.
32 J. P. M. Wielders and F. M. Everaerts, in B. J. Radola and D. Graesslin (Editors), *Electrofocusing and Isotachophoresis*, de Gruyter, Berlin, 1977, p. 527.
33 J. P. M. Wielders, *Thesis*, University of Technology, Eindhoven, 1978.
34 D. Kaniansky, M. Koval' and S. Stankoviansky, *J. Chromatogr.*, 267 (1983) 67.
35 F. M. Everaerts, Th. P. E. M. Verheggen and F. E. P. Mikkers, *J. Chromatogr.*, 169 (1978) 21.